Letter | Editors' Suggestion

Topological classification of one-dimensional chiral symmetric interfaces

Harry MullineauxSanders and Bernd Braunecker
SUPA, School of Physics and Astronomy, University of St. Andrews, North Haugh, St. Andrews KY16 9SS, United Kingdom

(Received 13 July 2024; revised 5 November 2024; accepted 4 December 2024; published 20 December 2024)

We address the topological classification of one-dimensional chiral symmetric interfaces embedded into a two-dimensional substrate. A proof of the validity of a topological classification based on the Green's function by explicit evaluation of the topological invariant is presented. Further, we show that due to entanglement between the in-gap modes and the substrate, the full physics of the substrate that is contained in the Green's function is required. This is done by considering a classification scheme derived from the reduced ground state projector, for which we show that an uncritical handling produces erroneous changes in the topological index due to entanglement driven gap closures. We illustrate our results by applying them to a tight-binding model of a spiral magnetic interface in a *s*-wave superconductor.

DOI: 10.1103/PhysRevB.110.L241409

Introduction. The realization of topological quantum states has been a major aim of condensed matter physics for a number of years. Most prominent is obtaining robust Majorana modes [1–3], as they would provide first steps toward topological quantum computation [4,5]. In the absence of intrinsic topological properties in a material [6], artificially created topological structures [7,8] have emerged as promising candidates for tunable topological states, and specifically chains of magnetic impurities on standard *s*-wave superconductors, have been of great interest recently.

Magnetic impurities locally break Cooper pairs [9,10] and create Yu-Shiba-Rusinov bound states [11–13]. Chains of impurities, such as shown in Fig. 1, create in-gap bands [12] which can be tuned to a topological phase through scattering strength and magnetic alignment. The topological properties of such magnetic interfaces have been determined by diagonalization of tight-binding models [8,9,14,15], by first principles calculation of Green's functions [16–18], by analytic determination of Green's functions with a Debye frequency cut-off [19], by effective tight-binding hybridization of impurity states [20–26], and by modeling one-dimensional (1D) magnetic wires with proximity induced superconductivity [27,28]. For densely packed chains, the effect of the reduced dimensionally of the embedded interface on band structure and topological has been investigated [29–33]. There has also been significant experimental effort in fabricating and studying these interfaces, some of which have shown signs of topological physics, however this evidence remains inconclusive [34–43].

As the topological properties are created at the interface, a characterization through effective 1D Hamiltonians obtained by tracing out the transverse spatial dimensions would be most convenient. However, this is only valid for in-gap modes tightly confined to the interface [31], and typically not realized in experiment [36]. Otherwise the bound modes have sufficient entanglement between the degrees of freedom in the unit cell and in space, such that essential information for topological classification is lost through spatial traces [31]. A usable 1D Hamiltonian must thus rely on a quantity that does not eliminate essential spatial information, and it has been proposed that this can be achieved through local Green's functions [31,32] yet only with circumstantial evidence.

In this paper, we prove that this approach is generally valid for any 1D interface embedded into a trivial substrate with a chiral symmetry under the assumption that the real space Green's function of the substrate contains no zeros. Thus, we provide a fast, versatile, and numerically and analytically tractable classification scheme. As an illustration we determine the topological phase diagram of a tight-binding model of a 1D magnetic interface in a two-dimensional (2D) superconductor. We demonstrate further that this method is resilient against the spatial entanglement of the bound states by comparing with the reduced ground state projector approach [44], and that the latter requires careful handling to avoid artifacts in the parameter regions of most interest.

Topological Hamiltonian. We consider a gapped translationally invariant 2D substrate with Hamiltonian $\mathcal{H}_0(k_x, k_y)$, for momenta k_x, k_y, with the gap centered about energy $\omega = 0$. A scattering interface is introduced as a strip along the x direction, bounded in the y direction. For simplicity, we assume the interface to be localized at $y = 0$, however generalization to wider interfaces is immediate by considering enhanced unit cells along y of the width of the interface. Assuming translational invariance along x, the scattering Hamiltonian is $\mathcal{H}_V(k_x) = H_V(k_x) \otimes P_{y=0}$, where $P_{y=0}$ projects onto the interface and H_V acts on the remaining degrees of freedom.

We denote by $g(\omega, k_x, y)$ the retarded Green's function at energy ω of $\mathcal{H}_0(k_x, k_y)$ after the partial Fourier transform $k_y \to y$. Then the total Green's function of $\mathcal{H} = \mathcal{H}_0 + \mathcal{H}_V$ with broken translational invariance in the y direction is given

Published by the American Physical Society under the terms of the Creative Commons Attribution 4.0 International license. Further distribution of this work must maintain attribution to the author(s) and the published article's title, journal citation, and DOI.

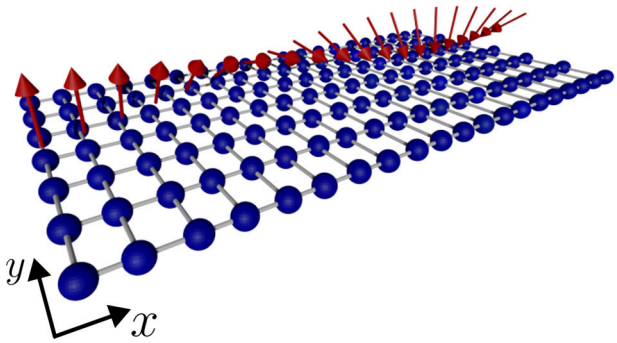


FIG. 1. Sketch of a spiral magnetic interface model: A square lattice tight-binding model of a s-wave superconducting substrate with a chain of spiralling magnetic impurities along the x direction.

by Dyson's equation [45]

$$G(\omega, k_x, y, y') = g(\omega, k_x, y - y') + g(\omega, k_x, y)T(\omega, k_x) \times g(\omega, k_x, -y'), \tag{1}$$

with the T matrix

$$T(\omega, k_x) = \left[H_V^{-1} - g(\omega, k_x, 0)\right]^{-1}. \tag{2}$$

The poles of $T(\omega, k_x)$ at fixed k_x provide the bound state energies, and their residues information on their wavefunctions. Consequently, T, and thus G, are expected to contain all topological information, and it was proposed [31,32] that

$$H^{\text{top}}(k_x, y) = -[G(\omega = 0, k_x, y, y)]^{-1} \tag{3}$$

forms at $y = 0$, a suitable topological Hamiltonian for topological classification. Similar Hamiltonians have been used for interacting topological materials [46–48].

We shall now prove that H^{top} is generally applicable for the topological classification for systems with chiral symmetries. This relies on the demonstration that H^{top} possesses the same global symmetries as the full 2D Hamiltonian. Let $\mathcal{H}(k_x)$ be the full Hamiltonian at fixed k_x, considered as a matrix acting on all other degrees of freedom including y. As $\mathcal{H}(k_x)$ is gapped, $G(\omega, k_x) = [\omega\mathbb{1} - \mathcal{H}(k_x)]^{-1}$ is nonsingular at $\omega = 0$. If $\tilde{\Lambda}$ is a symmetry operator such that $\tilde{\Lambda}\mathcal{H}(k_x)\tilde{\Lambda} = \pm\mathcal{H}(\pm k_x)$ for a given combination of $\pm$ signs, then $\tilde{\Lambda}G(0, k_x)\tilde{\Lambda} = \pm G(0, \pm k_x)$ holds as well [49]. If $\tilde{\Lambda}$ is global such that $\tilde{\Lambda} = \Lambda \otimes \mathbb{1}_y$ where $\mathbb{1}_y$ is the identity for the y coordinate and Λ acts on the remaining degrees of freedom [44], then it commutes with the projection onto y and

$$\Lambda^{-1}G(\omega = 0, k_x, y, y)\Lambda = \pm G(\omega = 0, \pm k_x, y, y). \tag{4}$$

Therefore, $H^{\text{top}}(k_x, y) = -[G(\omega = 0, k_x, y, y)]^{-1}$ satisfies all the global symmetries of the full Hamiltonian. Since furthermore the interface region is bounded in the y direction, the following theorem holds (see the SM [50]):

$$\mathcal{H} = \mathcal{H}_0 + \mathcal{H}_V \text{ possesses a global symmetry } \Lambda \otimes \mathbb{1}_y \Leftrightarrow \Lambda \text{ is a symmetry of } g(0, k_x, y) \text{ and } H_V \text{ individually.} \tag{5}$$

It follows from Eq. (2) that the T matrix also possesses the same symmetry. This means in any symmetry class, we can define a topological invariant individually for the topological Hamiltonian, the substrate Green's function, the T matrix and the scattering Hamiltonian. While the $\mathcal{H}(k_x)$ and $H^{\text{top}}(k_x, y)$ share the same symmetries, it is still possible for the topological Hamiltonian at a fine tuned y to have an enhanced symmetry which may effect the symmetry protection of its invariant.

We now specialize to chiral 1D symmetry classes which are relevant to magnetic impurity-superconductor interfaces [31,32,51]. In these classes, $\mathcal{H}(k_x)$ has a unitary Hermitian symmetry $\mathcal{C}$ such that $\mathcal{C}\mathcal{H}(k_x)\mathcal{C} = -\mathcal{H}(k_x)$. The appropriate topological invariant is the winding number, W, calculated by writing the H^{top} in the eigenbasis of $\mathcal{C}$ [52],

$$H^{\text{top}}(k_x, y) = \begin{pmatrix} 0 & h(k_x, y) \\ h^\dagger(k_x, y) & 0 \end{pmatrix}, \tag{6}$$

with $h(k_x, y)$ called the chiral decomposition, such that

$$W(y) = \frac{1}{2\pi i}\int_{-\pi}^{\pi} dk_x \partial_{k_x} \log\{\det[h(k_x, y)]\}. \tag{7}$$

Theorem (5) ensures that $g(\omega, k_x, y)$, $T(\omega = 0, k_x)$, and H_V individually admit simultaneous chiral decompositions as in Eq. (6). Since $H^{\text{top}}(k_x, y = 0) = -H_V T^{-1}(0, k_x)[g(0, k_x, 0)]^{-1}$, we obtain (see the SM [50])

$$W(y = 0) = W_{g^{-1}(y=0)} - W_{T^{-1}} + W_{H_V}, \tag{8}$$

which is the central result of this paper. Here W_A represents the winding number obtained from Eq. (7) with $h(k_x, y)$ replaced by the chiral decomposition of $A = [g(\omega = 0, k_x, y)]^{-1}$, $[T(\omega = 0, k_x)]^{-1}$, and H_V, respectively.

We note that $W_{g^{-1}(y=0)}$ can change its value only if a substrate pole passes through $\omega = 0$ or if the Green's function has a zero. The zeros do not reflect any gap closure of the full Hamiltonian and so create a fictitious phase boundary. However, previous work has suggested that such zeros of the partially Fourier transformed, in-gap Green's function are related to the topology of the substrate and are not present in trivial phases [53,54]. We shall proceed under the assumption that the substrate Green's function does not contain a zero.

For a trivial substrate in the absence of zeros and trivial (including on-site) scattering, $W_{g^{-1}(y=0)} = W_{H_V} = 0$, and therefore

$$W(y = 0) = -W_{T^{-1}}. \tag{9}$$

The invariant only becomes undefined and changes value when $\det\{[T(\omega = 0)]^{-1}\} = 0$, matching when the in-gap bands touch.

For a general H_V with k_x dependence, a gap closure could occur. These gap closures cause zeros in the T matrix and can change its winding number [49]. However, the relative negative sign between the two terms in Eq. (8) means any change caused by the appearance of such a zero is compensated by the change in winding number of the scattering Hamiltonian [50].

Based on these results, we prove in the Supplemental Material [50] that, for a trivial substrate without zeros, the topological Hamiltonian is trivial if and only if the Hamiltonian is trivial and as a consequence the the winding number of the Hamiltonian and topological Hamiltonian must be equal up to a possible sign that is global to the phase diagram. We

have therefore proven that for a trivial substrate, the topological Hamiltonian proposed in [31,32] provides the correct topological classification when y is tuned to the interface.

The classification in the case of a topologically nontrivial substrate via the topological Hamiltonian remains outstanding. H^{top} contains a dimensional reduction from a higher D dimensional substrate to a lower d dimensional interface. However, the allowed values of topological invariants change between dimensions [52] and symmetries allowing for a nontrivial system in D dimensions may impose only trivial states in d dimensions. Therefore $[g(\omega = 0, k_x, y)]^{-1}$ does not necessarily form a good topological Hamiltonian of the substrate, whereas a trivial state remains trivial after any dimensional reduction as it remains always amenable to the atomic limit. In addition, as proposed in Refs. [53,54], the substrate Green's function should generically have zero eigenvalues at some in-gap frequency. This reflects that at arbitrarily large scalar potential, an edge is created which should have a bound mode due to the bulk boundary correspondence. Such zeros could change the invariant of the topological Hamiltonian without a gap closure and could give inaccurate results.

When $y \neq 0$, the winding number becomes [50]

$$W(y) = W_{g^{-1}(y)} + W_{g^{-1}(-y)} - W_{T^{-1}} - \frac{1}{2\pi i}\int_{-\pi}^{\pi} dk\,\partial_k \times \log\{\det[\mathbb{1} + \tilde{g}^{-1}(-y)\tilde{T}^{-1\dagger}\tilde{g}^{-1}(y)\tilde{g}(0)]\}, \quad (10)$$

where $\tilde{g}^{-1}(y)$ and $\tilde{T}^{-1}$ are the chiral decompositions of $[g(\omega = 0, k_x, y)]^{-1}$ and $[T(\omega = 0, k_x)]^{-1}$, respectively. The final term can be singular and possess nontrivial winding. Indeed, as $|y| \to \infty$ the zeros of $G(\omega = 0, k_x, y, y)$ cancel the poles of $T(\omega = 0, k_x)$ (see the SM [50]) and the winding of the T matrix is perfectly canceled. Therefore $H^{\text{top}}(|y| \to \infty)$ is trivial, as observed already in Ref. [31]. As such, only $y = 0$ should be considered for topological classification as $y \neq 0$ or integrals over y may produce erroneous results.

Equation (8) is a general result applicable to any gapped substrate with any interface that has a chiral symmetry. Furthermore, it applies also to interfaces of larger width, by extending the matrix sizes to include the y coordinates of the interface too. The key appeal of this method is that it is calculated from analytically tractable objects, well defined in the system size $L \to \infty$ limit, removing any finite size effects. As only the local Green's function is required, this approach is applicable to first principals calculations [16–18,38]. It also opens the door to connecting this classification to local response functions that are experimentally accessible.

Application to magnetic interface in a superconductor. We demonstrate the usefulness of this approach with the topological classification of a chain of spiralling classical magnetic impurities embedded into a tight-binding model of a BCS (s-wave) superconductor, such as shown in Fig. 1. Similar to Refs. [8,21,23,30,31] we assume the impurities to form a scattering interface at $y = 0$ with planar magnetization $\mathbf{M}(x) = V_m(\cos(2k_m x), \sin(2k_m x), 0)$, where $V = V_m$ sets the scattering strength, and k_m the period of the spiral which is considered as a free parameter and not determined self-consistently [9,55–60]. Translational symmetry along x can be restored by a gauge transformation on the electron creation operator $c^\dagger_{x,y,\sigma} \to e^{ik_m\sigma x}c^\dagger_{x,y,\sigma}$, for spin $\sigma = \uparrow, \downarrow = +, -$ [61]. This maps the magnetization to $\mathbf{M} = V_m(1, 0, 0)$ but spin splits the bands by the shifts $k_x \to k_x + \sigma k_m$. In (k_x, y) space the components of the Hamiltonian $\mathcal{H} = \mathcal{H}_0 + \mathcal{H}_V$ are then written as

$$\mathcal{H}_0 = \sum_{k_x,y,\sigma}[-2t\cos(k_x + \sigma k_m) - \mu]c^\dagger_{k_x,y,\sigma}c_{k_x,y,\sigma} - t\sum_{k_x,y,\sigma}\left[\left(c^\dagger_{k_x,y+1,\sigma}c_{k_x,y,\sigma} + \Delta c^\dagger_{k_x,y,\uparrow}c^\dagger_{-k_x,y,\downarrow}\right) + \text{H.c.}\right], \quad (11)$$

and $\mathcal{H}_V = V_m\sum_{k_x} c^\dagger_{k_x,0,\uparrow}c_{k_x,0,\downarrow} + \text{H.c.}$, with hopping integral t, pairing Δ, and chemical potential μ. The coordinates x, y label a square lattice with lattice constant $a = 1$. We consider a constant Δ as this allows for an analytic solution for the phase boundaries, and as its self-consistent adjustment near the impurities has little effect [50]. We finally note that the substrate Green's function cannot have a zero for any nonzero Δ.

For $k_m \neq n\pi$ where $n \in \mathbb{Z}$, the model is in the BDI symmetry class [52], with chiral $\mathcal{C} = \tau^y\sigma^x$, particle-hole $\mathcal{P} = i\tau^x K$, time reversal $\mathcal{T} = \tau^z\sigma^x K$, and inversion symmetry $\mathcal{I} = \tau^z\sigma^x$ operators [62], for spin σ^i and particle-hole τ^i Pauli matrices, and complex conjugation K. The calculation of $g(\omega, k_x, y)$ follows Ref. [30] (see [50]), from which we obtain $T(\omega, k_x)$. The poles of $T(0, k_x)$ provide the gap closures of the in-gap bands that mark the topological phase boundaries, and occur at the high symmetry points $k_x = 0, \pi$ for the scattering strengths [50]

$$V^*_{m,k_x} = \pm\{[g^\uparrow_{11}(k_x)]^2 + [g^\uparrow_{12}(k_x)]^2\}^{-1/2}, \quad (12)$$

where $g^\uparrow_{11}$ and $g^\uparrow_{12}$ are the (↑,particle)-(↑,particle) and (↑,particle)-(↓,hole) terms of $g(\omega = 0, k_x, y = 0)$. In the continuum limit, $V^*_{m,k_x=0}$ reproduces the result of Ref. [31]. Gap closures occur only at $k_x = 0, \pi$, and so W is restricted to $W = 0, \pm 1$. Using H^{top} and Eq. (9) the parity of W can be written as [51]

$$(-1)^{W(y=0)} = \prod_{k_x=0,\pi}\text{sign}\left[\left(V^*_{m,k_x}\right)^{-2} - (V_m)^{-2}\right], \quad (13)$$

and the phase is nontrivial for $\min(V^*_{m,k_x=0}, V^*_{m,k_x=\pi}) < V_m < \max(V^*_{m,k_x=0}, V^*_{m,k_x=\pi})$. If instead $k_m = n\pi$, the spin sectors decouple and $\mathcal{H}$ block diagonalizes into two s-wave Hamiltonians with each block subject to a local Zeeman shift $V_m\sigma^z$. Each block is in the trivial CI class such that always $W = 0$ [52].

The resulting phase diagram is shown in Fig. 2(a). To further corroborate our results, in Fig. 2(b) we show the entanglement spectrum $\tilde{\zeta}$ as V_m is varied along the vertical dashed line in Fig. 2(a) obtained from an entanglement cut made perpendicular to the chain [63–65]. The entanglement spectrum is defined as the spectrum of the ground state projector $P_{GS} = \sum_{E_N<0}|E_N\rangle\langle E_N|$ for eigenstates of the Hamiltonian $|E_N\rangle$ whose gap quantifies the degree of entanglement between two halves of the system. An edge is introduced into the system by restricting the position index to one half of the system. In a trivial phase $\tilde{\zeta}$ is gapped about $1/2$, whereas in a nontrivial phase there is a doubly degenerate value $\tilde{\zeta} = 1/2$ [63]. This matches exactly our phase diagram.

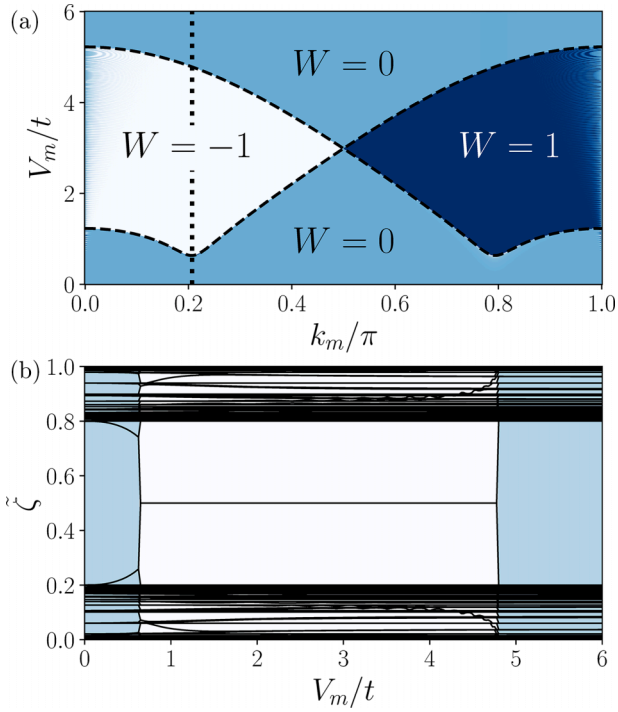


FIG. 2. (a) Winding number of $H^{\text{top}}(k_x, y = 0)$, with values represented by the background color, for $\Delta = 0.1t$ and $k_F = 0.65$. Black dashed lines show the phase boundaries [Eq. (12)]. At $k_m = 0, \pi$ the model is gapless and changes symmetry class. The fuzzy pattern nearby arises from numerical instabilities caused by tiny gaps. The minima of the lower phase boundary are at $k_m = k_F, \pi - k_F$. (b) Entanglement spectrum $\tilde{\zeta}$ at $k_m = k_F$ for V_m varying along the dotted line in (a), computed for a 50×101 lattice with an entanglement cut made perpendicular to the impurity chain splitting the system in two. The background color is as in (a). Edge modes, characterized by $\tilde{\zeta} = 1/2$, appear exactly when the winding number of the topological Hamiltonian is nontrivial.

Classification of magnetic interface model via reduced projector. The topological Hamiltonian is a local probe, but through G contains information on the entire band structure, not just on the in-gap states. It may thus be natural to ask how much involvement of the extended substrate states is required, and whether the topological properties are reproducible from the wavefunctions truncated to a small wedge around the interface. To provide an answer, we compare with the classification scheme proposed in Ref. [44] under spatial truncation for a D dimensional trivial substrate with embedded $d < D$ dimensional topological model. If $|GS\rangle$ is the ground state, the classification is based on the projector [64]

$$P^{\alpha,\beta}_{i,j}(k) = \langle GS| c^{\dagger}_{k,i,\alpha} c_{k,j,\beta} |GS\rangle , \tag{14}$$

where k is the d dimensional momentum in the translationally invariant directions, i, j label the further spatial coordinates, and α, β the unit cell degrees of freedom. Spatial degrees of freedom can be traced out by restricting the projector to a spatial region $\mathcal{R}$ that contains the embedded system. This leaves a reduced projector $P^{\mathcal{R}}(k)$ [65] with eigenvalues $\zeta_i(k) \in [0, 1]$ and eigenvectors $|\zeta_i(k)\rangle$. The value ζ_i weights how much the eigenstate is supported in $\mathcal{R}$. The crossing through $\zeta = 1/2$ thus indicates a qualitative change of the entanglement between $\mathcal{R}$ and its complement, and the possible topological implication can be captured through the entanglement projector [44] $\Pi^{\mathcal{R}}(k) = \sum_{\zeta_i(k)>1/2} |\zeta_i(k)\rangle \langle\zeta_i(k)|$, which is in the same symmetry class as the Hamiltonian [44], such that $1 - 2\Pi^{\mathcal{R}}(k)$ acts like a spectrally flattened band Hamiltonian with generally a gap about zero and allows for the standard extraction of topological invariants [52].

However, changes of the reduced projector's invariants do not necessarily match topological phase transitions. Such changes can also be caused by gap closures due to entanglement between $\mathcal{R}$ and its complement from sufficiently extended in-gap states, and not only by gap closures of $\mathcal{H}$. Indeed, in Fig. 3(a) we show the winding number of $1 - 2\Pi^{\mathcal{R}}$ for the magnetic interface model [66], with $\mathcal{R}$ reduced to just one site at $y = 0$. The result does not match Fig. 2(a), overshooting the phase boundary for $k_m \approx 0$ and undershooting for $k_m \approx k_F$, as shown in the close up of Fig. 3(b). This error is reproduced for larger lattice sizes and in the entanglement spectrum, and only by enlarging $\mathcal{R}$ to a width of ≈6 sites the correct phase diagram is recovered. The error is particularly significant as $k_m = k_F$ is of much interest for self-sustained magnetic spirals [9,55–58].

The projector's invariant can change if the projector is discontinuous or its gap closes. The former occurs when the Hamiltonian's gap closes and the ground state reconfigures. The latter is associated with $\zeta = 1/2$ and represents maximal entanglement through maximization of the entropy $S = -\zeta \log(\zeta)$ [67]. Such modes occur when the in-gap wavefunctions spread across $\mathcal{R}$ and have strong correlation between y and spin-Nambu degrees of freedom [31]. Figure 3(c) shows they are indeed responsible for the erroneous phase diagram. That lower dimensional subsystems of gapped systems can become gapless has previously been reported in Dirac systems [68].

The ground state projector classification therefore requires careful checking of the extent of the localized wavefunctions. Alternatively, every phase transition predicted by this method would need to be checked as to whether it is due to gap closing in the Hamiltonian or in the reduced projector. Both could become computationally costly. This underlines the significance of the role of the substrate in the dimensional reduction that is captured by a Green's function based method as put forward in this paper.

Conclusions. We have shown that the topological classification of 1D interfaces embedded into a topologically trivial 2D substrate with chiral symmetry can be performed exactly by the local Green's function tuned to the interface. With Eq. (8) we provide an explicit formula disentangling the local scattering effects from the substrate, while maintaining the full spatial dependence of the substrate through the T matrix. The topological Hamiltonian provides a very fast, analytically and numerically tractable classification, free of finite size effects or scaling with the size of the substrate. While it is necessary to assume that the substrate Green's function contains no zeros, previous work suggests this is generically true for a trivial substrate. The same studies suggest that zeros are generically present for topological substrates, complicating the classification of interfaces embedded into nontrivial substrates. We demonstrate further

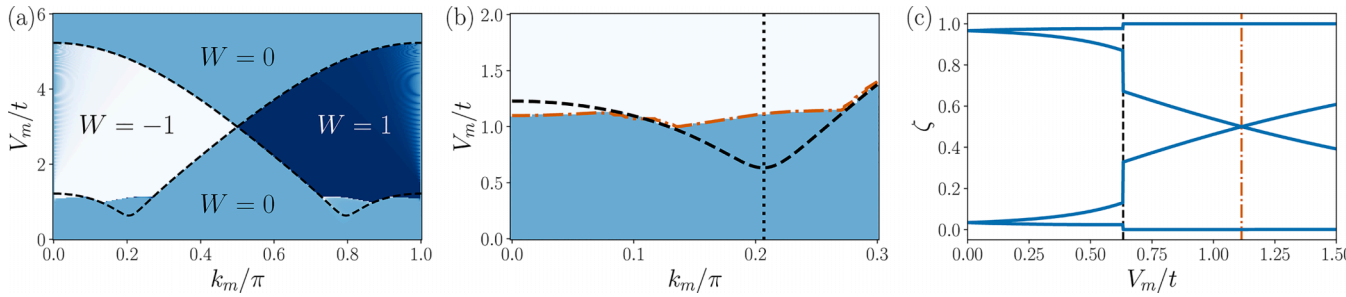


FIG. 3. (a) Winding number of $1 - 2\Pi^{\mathcal{R}}$, the projector restricted to the impurity site at $y = 0$, for $N_y = 101$, $k_F = 0.65$, and $\Delta = 0.1t$. The black dashed lines show the phase boundaries [Eq. (12)]. The classification gives the incorrect topological invariant, overshooting the phase boundary for $k_m \approx 0$ and undershooting it for $k_m \approx k_F$. The fuzzy pattern $k_m a = 0, \pi$ arises from numerical instability near gap closures. (b) Same as (a) zoomed on $k_m \approx k_F$. The orange dash-dotted line shows where the gap of the projector closes, matching exactly where the winding number changes. (c) Entanglement spectrum ζ of the projector $P^{\mathcal{R}}$ reduced to just $y = 0$, at $k_x = 0$, $k_m = k_F$ as V_m is varied along the dotted line in (b). The black dashed and orange dash-dotted lines mark the boundaries as in (b). The discontinuity in ζ (black line) mark the true phase transition, whereas the erroneous phase transition by the projector appears where the ζ gap closes instead (orange line).

that the full spatial dependence is crucial for the classification, and care must be taken when using classification schemes relying on spatial truncation. The proof of the applicability of a local Green's function classification to nonchiral symmetry classes and higher dimensions requiring Pfaffian or Chern invariants remains outstanding, but we believe such extensions are possible. A proof for Pfaffian invariants in 1D would cover class D superconductors and complete the classification of all nontrivial 1D symmetry classes [52,69].

Acknowledgments. The authors thank Joe Winter and Konner McNeillie for helpful discussions. H.M.S. acknowledges studentship funding from EPSRC under Grant No. EP/W524505/1. The work presented in this paper is theoretical. No data were produced, and supporting research data are not required.

[1] A. Y. Kitaev, Unpaired Majorana fermions in quantum wires, Phys. Usp. **44**, 131 (2001).
[2] N. Read and D. Green, Paired states of fermions in two dimensions with breaking of parity and time-reversal symmetries and the fractional quantum Hall effect, Phys. Rev. B **61**, 10267 (2000).
[3] M. Sato and Y. Ando, Topological superconductors: A review, Rep. Prog. Phys. **80**, 076501 (2017).
[4] A. Y. Kitaev, Fault-tolerant quantum computation by anyons, Ann. Phys. **303**, 2 (2003).
[5] J. K. Pachos, *Introduction to Topological Quantum Computation* (Cambridge University Press, Cambridge, 2012).
[6] M. M. Sharma, P. Sharma, N. K. Karn, and V. P. S. Awana, Comprehensive review on topological superconducting materials and interfaces, Supercond. Sci. Technol. **35**, 083003 (2022).
[7] Y. Oreg, G. Refael, and F. von Oppen, Helical liquids and Majorana bound states in quantum wires, Phys. Rev. Lett. **105**, 177002 (2010).
[8] S. Nadj-Perge, I. K. Drozdov, B. A. Bernevig, and A. Yazdani, Proposal for realizing Majorana fermions in chains of magnetic atoms on a superconductor, Phys. Rev. B **88**, 020407(R) (2013).
[9] I. Reis, D. J. J. Marchand, and M. Franz, Self-organized topological state in a magnetic chain on the surface of a superconductor, Phys. Rev. B **90**, 085124 (2014).
[10] T. Meng, J. Klinovaja, S. Hoffman, P. Simon, and D. Loss, Superconducting gap renormalization around two magnetic impurities: From Shiba to Andreev bound states, Phys. Rev. B **92**, 064503 (2015).
[11] L. Yu, Bound state in superconductors with paramagnetic impurities, Acta Phys. Sin. **21**, 75 (1965).
[12] H. Shiba, Classical spins in superconductors, Prog. Theor. Phys. **40**, 435 (1968).
[13] A. I. Rusinov, Superconductivity near a paramagnetic impurity, Zh. Eksp. Teor. Fiz. Pisma Red. **9**, 146 (1968) [JETP Lett. **9**, 85 (1969)].
[14] M. H. Christensen, M. Schecter, K. Flensberg, B. M. Andersen, and J. Paaske, Spiral magnetic order and topological superconductivity in a chain of magnetic adatoms on a two-dimensional superconductor, Phys. Rev. B **94**, 144509 (2016).
[15] J. Li, H. Chen, I. K. Drozdov, A. Yazdani, B. A. Bernevig, and A. H. MacDonald, Topological superconductivity induced by ferromagnetic metal chains, Phys. Rev. B **90**, 235433 (2014).
[16] B. Nyári, A. Lászlóffy, G. Csire, L. Szunyogh, and B. Újfalussy, Topological superconductivity from first principles. I. Shiba band structure and topological edge states of artificial spin chains, Phys. Rev. B **108**, 134512 (2023).
[17] A. Lászlóffy, B. Nyári, G. Csire, L. Szunyogh, and B. Újfalussy, Topological superconductivity from first principles. II. Effects from manipulation of spin spirals: Topological fragmentation, braiding, and quasi-Majorana bound states, Phys. Rev. B **108**, 134513 (2023).
[18] D. Sticlet and C. Morari, Topological superconductivity from magnetic impurities on monolayer $NbSe_2$, Phys. Rev. B **100**, 075420 (2019).
[19] C. Mier, D.-J. Choi, and N. Lorente, Calculations of in-gap states of ferromagnetic spin chains on s-wave wide-band superconductors, Phys. Rev. B **104**, 245415 (2021).
[20] T.-P. Choy, J. M. Edge, A. R. Akhmerov, and C. W. J. Beenakker, Majorana fermions emerging from magnetic

nanoparticles on a superconductor without spin-orbit coupling, Phys. Rev. B **84**, 195442 (2011).
[21] F. Pientka, L. I. Glazman, and F. von Oppen, Topological superconducting phase in helical Shiba chains, Phys. Rev. B **88**, 155420 (2013).
[22] F. Pientka, L. I. Glazman, and F. von Oppen, Unconventional topological phase transitions in helical Shiba chains, Phys. Rev. B **89**, 180505(R) (2014).
[23] A. Weststrom, K. Pöyhönen, and T. Ojanen, Topological properties of helical Shiba chains with general impurity strength and hybridization, Phys. Rev. B **91**, 064502 (2015).
[24] P. M. R. Brydon, S. Das Sarma, H.-Y. Hui, and J. D. Sau, Topological Yu-Shiba-Rusinov chain from spin-orbit coupling, Phys. Rev. B **91**, 064505 (2015).
[25] A. Heimes, P. Kotetes, and G. Schön, Majorana fermions from Shiba states in an antiferromagnetic chain on top of a superconductor, Phys. Rev. B **90**, 060507(R) (2014).
[26] K. Pöyhönen, A. Weststrom, and T. Ojanen, Topological superconductivity in ferromagnetic atom chains beyond the deep-impurity regime, Phys. Rev. B **93**, 014517 (2016).
[27] G. M. Andolina and P. Simon, Topological properties of chains of magnetic impurities on a superconducting substrate: Interplay between the Shiba band and ferromagnetic wire limits, Phys. Rev. B **96**, 235411 (2017).
[28] Y. Peng, F. Pientka, L. I. Glazman, and F. von Oppen, Strong localization of Majorana end states in chains of magnetic adatoms, Phys. Rev. Lett. **114**, 106801 (2015).
[29] Q.-H. Wang and Z. D. Wang, Impurity and interface bound states in $d_{x^2-y^2} + id_{xy}$ and $p_x + ip_y$ superconductors, Phys. Rev. B **69**, 092502 (2004).
[30] C. J. F. Carroll and B. Braunecker, Subgap states at ferromagnetic and spiral-ordered magnetic chains in two-dimensional superconductors. I. Continuum description, Phys. Rev. B **104**, 245133 (2021).
[31] C. J. F. Carroll and B. Braunecker, Subgap states at ferromagnetic and spiral-ordered magnetic chains in two-dimensional superconductors. II. Topological classification, Phys. Rev. B **104**, 245134 (2021).
[32] N. Sedlmayr, V. Kaladzhyan, and C. Bena, Analytical and semi-analytical tools to determine the topological character of Shiba chains, Phys. Rev. B **104**, 024508 (2021).
[33] N. Sedlmayr and C. Bena, Instability of Majorana states in Shiba chains due to leakage into a topological substrate, J. Phys.: Condens. Matter **34**, 104004 (2022).
[34] S. Nadj-Perge, I. K. Drozdov, J. Li, H. Chen, S. Jeon, J. Seo, A. H. MacDonald, B. A. Bernevig, and A. Yazdani, Observation of Majorana fermions in ferromagnetic atomic chains on a superconductor, Science **346**, 602 (2014).
[35] M. Ruby, F. Pientka, Y. Peng, F. von Oppen, B. W. Heinrich, and K. J. Franke, End states and subgap structure in proximity-coupled chains of magnetic adatoms, Phys. Rev. Lett. **115**, 197204 (2015).
[36] G. C. Ménard, S. Guissart, C. Brun, S. Pons, V. S. Stolyarov, F. Debontridder, M. V. Leclerc, E. Janod, L. Cario, D. Roditchev, P. Simon, and T. Cren, Coherent long-range magnetic bound states in a superconductor, Nat. Phys. **11**, 1013 (2015).
[37] R. Pawlak, M. Kisiel, J. Klinovaja, T. Meier, S. Kawai, T. Glatzel, D. Loss, and E. Meyer, Probing atomic structure and Majorana wavefunctions in mono-atomic Fe chains on superconducting Pb surface, npj Quantum Inf. **2**, 16035 (2016).
[38] B. E. Feldman, M. T. Randeria, J. Li, S. Jeon, Y. Xie, Z. Wang, I. K. Drozdov, B. Andrei Bernevig, and A. Yazdani, High-resolution studies of the Majorana atomic chain platform, Nat. Phys. **13**, 286 (2017).
[39] M. Ruby, B. W. Heinrich, Y. Peng, F. von Oppen, and K. J. Franke, Exploring a proximity-coupled Co chain on Pb(110) as a possible Majorana platform, Nano Lett. **17**, 4473 (2017).
[40] L. Schneider, P. Beck, J. Neuhaus-Steinmetz, L. Rózsa, T. Posske, J. Wiebe, and R. Wiesendanger, Precursors of Majorana modes and their length-dependent energy oscillations probed at both ends of atomic Shiba chains, Nat. Nanotechnol. **17**, 384 (2022).
[41] E. Liebhaber, L. M. Rütten, G. Reecht, J. F. Steiner, S. Rohlf, K. Rossnagel, F. von Oppen, and K. J. Franke, Quantum spins and hybridization in artificially-constructed chains of magnetic adatoms on a superconductor, Nat. Commun. **13**, 2160 (2022).
[42] H. Kim, A. Palacio-Morales, T. Posske, L. Rózsa, K. Palotás, L. Szunyogh, M. Thorwart, and R. Wiesendanger, Toward tailoring Majorana bound states in artificially constructed magnetic atom chains on elemental superconductors, Sci. Adv. **4**, eaar5251 (2018).
[43] L. Schneider, S. Brinker, M. Steinbrecher, J. Hermenau, T. Posske, M. dos Santos Dias, S. Lounis, R. Wiesendanger, and J. Wiebe, Controlling in-gap end states by linking nonmagnetic atoms and artificially-constructed spin chains on superconductors, Nat. Commun. **11**, 4707 (2020).
[44] T. I. Tuegel, V. Chua, and T. L. Hughes, Embedded topological insulators, Phys. Rev. B **100**, 115126 (2019).
[45] E. N. Economou, *Green's Functions in Quantum Physics*, Springer Series in Solid-State Sciences, Vol. 7 (Springer Berlin Heidelberg, Berlin, Heidelberg, 2006).
[46] G. E. Volovik, *The Universe in a Helium Droplet*, 1st ed. (Oxford University Press, Oxford, 2009).
[47] Z. Wang and S.-C. Zhang, Simplified topological invariants for interacting insulators, Phys. Rev. X **2**, 031008 (2012).
[48] Z. Wang and B. Yan, Topological Hamiltonian as an exact tool for topological invariants, J. Phys.: Condens. Matter **25**, 155601 (2013).
[49] V. Gurarie, Single-particle Green's functions and interacting topological insulators, Phys. Rev. B **83**, 085426 (2011).
[50] See Supplemental Material at http://link.aps.org/supplemental/10.1103/PhysRevB.110.L241409 for detailed proofs and calculations.
[51] S. Tewari and J. D. Sau, Topological invariants for spin-orbit coupled superconductor nanowires, Phys. Rev. Lett. **109**, 150408 (2012).
[52] C.-K. Chiu, J. C. Teo, A. P. Schnyder, and S. Ryu, Classification of topological quantum matter with symmetries, Rev. Mod. Phys. **88**, 035005 (2016).
[53] R.-J. Slager, L. Rademaker, J. Zaanen, and L. Balents, Impurity-bound states and Green's function zeros as local signatures of topology, Phys. Rev. B **92**, 085126 (2015).
[54] S.-S. Diop, L. Fritz, M. Vojta, and S. Rachel, Impurity bound states as detectors of topological band structures revisited, Phys. Rev. B **101**, 245132 (2020).
[55] B. Braunecker and P. Simon, Interplay between classical magnetic moments and superconductivity in quantum one-dimensional conductors: Toward a self-sustained topological Majorana phase, Phys. Rev. Lett. **111**, 147202 (2013).

[56] Y. Kim, M. Cheng, B. Bauer, R. M. Lutchyn, and S. Das Sarma, Helical order in one-dimensional magnetic atom chains and possible emergence of Majorana bound states, Phys. Rev. B **90**, 060401(R) (2014).

[57] J. Klinovaja, P. Stano, A. Yazdani, and D. Loss, Topological superconductivity and Majorana fermions in RKKY systems, Phys. Rev. Lett. **111**, 186805 (2013).

[58] M. M. Vazifeh and M. Franz, Self-organized topological state with Majorana fermions, Phys. Rev. Lett. **111**, 206802 (2013).

[59] M. Schecter, M. S. Rudner, and K. Flensberg, Spin-lattice order in one-dimensional conductors: Beyond the RKKY effect, Phys. Rev. Lett. **114**, 247205 (2015).

[60] M. Schecter, K. Flensberg, M. H. Christensen, B. M. Andersen, and J. Paaske, Self-organized topological superconductivity in a Yu-Shiba-Rusinov chain, Phys. Rev. B **93**, 140503(R) (2016).

[61] B. Braunecker, G. I. Japaridze, J. Klinovaja, and D. Loss, Spin-selective Peierls transition in interacting one-dimensional conductors with spin-orbit interaction, Phys. Rev. B **82**, 045127 (2010).

[62] D. Varjas, T. Ö. Rosdahl, and A. R. Akhmerov, Qsymm: algorithmic symmetry finding and symmetric Hamiltonian generation, New J. Phys. **20**, 093026 (2018).

[63] T. L. Hughes, E. Prodan, and B. A. Bernevig, Inversion-symmetric topological insulators, Phys. Rev. B **83**, 245132 (2011).

[64] I. Peschel, Calculation of reduced density matrices from correlation functions, J. Phys. A: Math. Gen. **36**, L205 (2003).

[65] A. Alexandradinata, T. L. Hughes, and B. A. Bernevig, Trace index and spectral flow in the entanglement spectrum of topological insulators, Phys. Rev. B **84**, 195103 (2011).

[66] L. Fidkowski, Entanglement spectrum of topological insulators and superconductors, Phys. Rev. Lett. **104**, 130502 (2010).

[67] S. Ryu and Y. Hatsugai, Entanglement entropy and the Berry phase in the solid state, Phys. Rev. B **73**, 245115 (2006).

[68] A. G. Moghaddam, K. Pöyhönen, and T. Ojanen, Boiling quantum vacuum: Thermal subsystems from ground-state entanglement, PRX Quantum **3**, 030335 (2022).

[69] J. C. Budich and E. Ardonne, Equivalent topological invariants for one-dimensional Majorana wires in symmetry class D, Phys. Rev. B **88**, 075419 (2013).